

# Taking measure of the Andromeda halo: a kinematic analysis of the giant stream surrounding M 31

R. Ibata<sup>1</sup>, S. Chapman<sup>2</sup>, A. M. N. Ferguson<sup>3</sup>, M. Irwin<sup>4</sup>, G. Lewis<sup>5</sup>, A. M. Connachie<sup>4</sup>

<sup>1</sup> Observatoire de Strasbourg, 11, rue de l'Université, F-67000, Strasbourg, France

<sup>2</sup> California Institute of Technology, Pasadena, CA 91125, U.S.A

<sup>3</sup> Max-Planck Institut für Astrophysik, Karl-Schwarzschild-Str. 1, Postfach 1317, D-85741, Garching, Germany

<sup>4</sup> Institute of Astronomy, Madingley Road, Cambridge, CB3 0HA, U.K.

<sup>5</sup> Institute of Astronomy, School of Physics, A29, University of Sydney, NSW 2006, Australia

20 March 2024

## ABSTRACT

We present a spectroscopic survey of the giant stellar stream found in the halo of the Andromeda galaxy. Taken with the DEMOS multi-object spectrograph on the Keck2 telescope, these data display a narrow velocity dispersion of  $11.3 \text{ km s}^{-1}$ , with a steady radial velocity gradient of  $245 \text{ km s}^{-1}$  over the 125 kpc radial extent of the stream studied so far. This implies that the Andromeda galaxy possesses a substantial dark matter halo. We test the orbit of the stream in different galaxy potential models. In a simple model with a composite bulge, disk and halo, where the halo follows a "universal" profile that is compressed by the formation of the baryonic components, we find that the kinematics of the stream require a total mass inside 125 kpc of  $M_{125} = 7.5^{+2.5}_{-1.3} \times 10^{11} M_{\odot}$ , or  $M_{125} > 5.4 \times 10^{11} M_{\odot}$  at the 99% confidence level. This is the first galaxy in which it has been possible to measure the halo mass distribution by such direct dynamical means over such a large distance range. The resulting orbit shows that if M 32 or NGC 205 are connected with the stream, they must either trail or lag the densest region of the stream by more than 100 kpc. Furthermore, according to the best-fit orbit, the stream passes very close to M 31, causing its demise as a coherent structure and producing a fan of stars that will pollute the inner halo, thereby confusing efforts to measure the properties of genuine halo populations. Our data show that several recently identified planetary nebulae, which have been proposed as evidence for the existence of a new companion of M 31, are likely members of the Andromeda Stream.

## 1 INTRODUCTION

Stellar streams represent the visible remnants of the merging process by which the halos of galaxies are built up. By studying these streams we can attempt to unravel the formation of galactic halos, seeing when, how and how many small galaxies arrived and were incorporated into large galaxies (Helmi & White 1999; Johnston, Sackett & Bullock 2001). Streams are also of great interest as probes of the large-scale mass distribution of the dark halos they reside in (Johnston et al. 1999; Ibata et al. 2001a; Zhao et al. 1999). This utility stems from the fact that streams from low-mass disrupting stellar systems trace the orbit of their progenitor, giving a means to constrain the tangential motion of the stars in the stream. The stars must move along the stream, and the magnitude of the tangential velocity must be such that, when the star is integrated along the orbit, it ends up with the same velocity as the stars that are currently downstream on the same orbit.

Giant stellar streams may well be common structures around galaxies (Pohlen et al. 2003; Malin & Hadley 1997). Indeed, the most conspicuous feature in the halo of the Milky Way is the giant rosette stream originating from the Sagittarius

dwarf galaxy, which contains approximately half of the high latitude ( $|b| > 30^\circ$ ) intermediate age stars at distances greater than 15 kpc (Ibata et al. 2001a, 2002; Majewski et al. 2003). It would appear that the Milky Way has not incorporated into the Halo a more massive galaxy than the Sagittarius dwarf over the last  $\sim 7 \text{ Gyr}$ .

This naturally leads to the question of whether the MW has unusual feeding habits. To answer this, we have undertaken a large photometric study of M 31, using the wide field cameras at the INT and CFHT telescopes to resolve stars over the entire disk and inner halo of that galaxy (Ibata et al. 2001b; Ferguson et al. 2002; M Connachie et al. 2003). This has given us an unprecedented panoramic view of the large scale and small scale structure of a disk galaxy. The analysis of this huge dataset is still in progress, but it has already yielded some surprising results regarding the incidence of substructure in the halo of M 31. The most prominent of these substructures is a stream-like over-density of stars near the minor axis of M 31 (Ibata et al. 2001b), at first sight a facsimile of the Sagittarius Stream around the Milky Way. The red giant branch (RGB) stellar density in the halo increases on average by a factor of two in the on-stream regions and is statistically significant at the 50-sigma level. Inter-

arXiv:astro-ph/0403068v1 2 Mar 2004

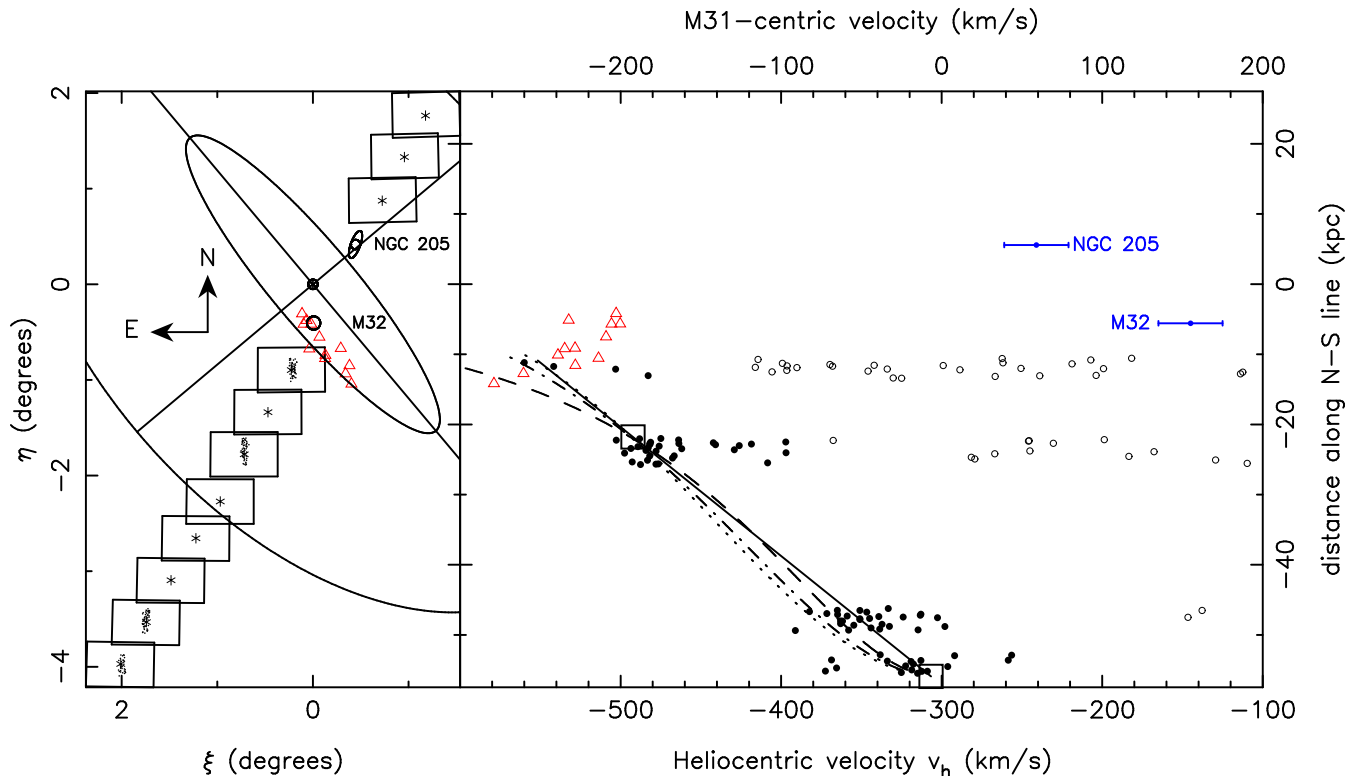


Figure 1. The left hand panel shows the locations of the observed fields on the plane of the sky, in standard coordinates  $(\xi; \eta)$ . Asterisk symbols denote field centres of, from South to North, Fields 1 (8 and 12) (14 of our photometric survey of the Andromeda Stream with the CFHT 12K camera; while the large rectangles display the size of the CFHT 12K camera pointings. The Keck2 DEIMOS targets are shown as small dots in the centre of Fields 1, 2, 6 and 8. Triangles represent the positions of the planetary nebulae identified by Morrison et al. (2003). The inner ellipse demarcates the approximate limit of the visible disk of M 31 at  $2r$  ( $r = 27$  kpc radius), and the outer ellipse shows a segment of a 50 kpc radius ellipse attenuated to  $c=a = 0.6$ , corresponding to the approximate limit of our INT survey. The right hand panel presents the radial velocity measurements (full circles), as a function of distance from M 31 along the declination direction ( $r = 780 \tan(\eta)$  kpc). The positions of M 32 and NGC 205 are also shown. The black line shows a straight-line fit [ $v_h(\eta) = 4244.8 \tan(\eta) - 610.9$  km s $^{-1}$ ] to the high negative velocity edge of this diagram. Stars that are more than 100 km s $^{-1}$  away from this line are marked with open circles. The two large squares show the chosen points for our "back-of-the-envelope" calculation, detailed in Section 3. The dashed, dot-dashed and dotted lines show the orbital paths in simple Kepler, logarithmic and NFW potentials, respectively. The velocities of the Morrison et al. (2003) PNe are represented again with triangles.

estingly, this stream points toward the Andromeda satellites M 32 and NGC 205, and is aligned with the outer isophotes of NGC 205, suggesting a relationship between the Andromeda Stream and these two dwarf galaxies. If this interpretation is correct, the stream has to be the result of previous interactions with M 31, as there is otherwise not enough time to spatially separate it from either of the two dwarf galaxies.

The proximity of M 31 provides us with an opportunity to undertake a spectroscopic survey of individual stars within the stream; indeed Andromeda offers the only extragalactic giant galaxy in which such a study can be undertaken with current instrumentation, as in more distant systems such halo substructure would be smeared into very low surface brightness features.

One useful property of the stream is that it is on a highly radial orbit. It passes very close to the centre of M 31, where a comparison of the RGB tip of the stream with that of M 31 itself shows them to lie at the same distance (McConnachie et al. 2003); whereas in the furthest field that it has been detected to date, the peak of its giant branch is 0.27 mag fainter, indicating that it is 106  $\pm$  20 kpc behind M 31 (McConnachie et al. 2003). This fortuitous alignment

close to the line of sight, allows us to measure directly the potential gradient over  $> 100$  kpc, and hence measure the halo mass.

The layout of this paper is as follows: section 2 presents the spectroscopic survey of the Andromeda Stream, the results of which are used in section 3 to constrain the mass of the dark matter halo of M 31, and finally in section 4 we discuss the significance of the results and present the conclusions of this study. Throughout this work, we assume a distance of 780 kpc to M 31 (Stanek & Gamavich 1998) and a systemic radial velocity of 300 km s $^{-1}$  (de Vaucouleurs et al. 1991).

## 2 THE ANDROMEDA HALO SURVEY

To understand the nature of the substructures detected in our panoramic halo surveys of M 31, we undertook a follow-up programme to measure the kinematics of individual RGB stars with the DEIMOS spectrograph on the Keck2 10m telescope. On Sep 29-30 2002, we used the instrument in the high-resolution configuration with the 1200nm grat-

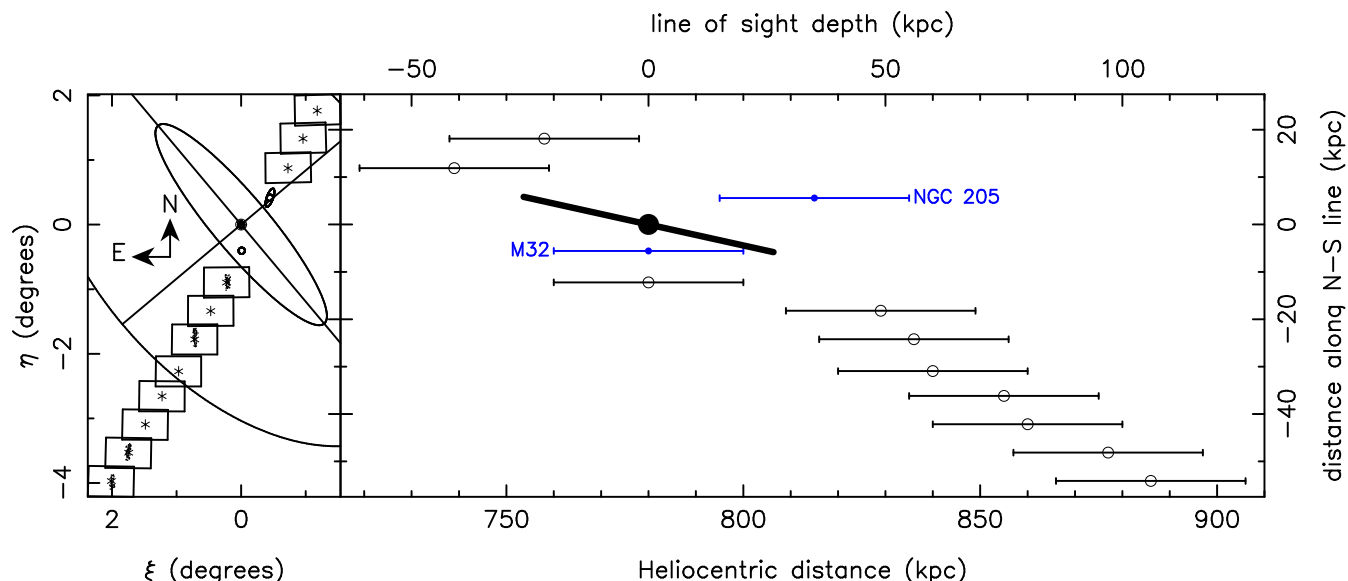


Figure 2. For convenience, the left-hand panel reproduces the chart shown previously in Figure 1. The right-hand panel shows a sideways view of the stream, drawn to the same scale as the left-hand panel, which displays the line of sight depth of the fields, together with the positions of M 32 and NGC 205. The disk of M 31 is highly inclined to our line of sight ( $12.5^\circ$ ); the thick line is a schematic representation of a disk of radius 27 kpc inclined at  $12.5^\circ$ . Evidently the stream orbits close to the plane of the Andromeda galaxy.

ing (giving access to the spectral region 6400 Å to 9000 Å) to obtain high quality spectra of 768 stars in 9 fields in M 31. This has given an order of magnitude improvement in statistics over previous radial velocity surveys of the M 31 system Reitzel & Guhathakurta (2002). The present contribution examines data from four fields along the giant stellar stream.

Red giant branch stars were selected for observation from our CFHT 12K camera survey, which covers the region of the sky shown schematically on the left-hand panel of Figure 1. Stars were selected by choosing point-sources with I-band magnitudes between  $20.5 < I < 22.0$  and colours  $1.0 < V - I < 4.0$ . Both metal-poor and metal-rich populations will be present in this selection region (see e.g. McConnachie et al. 2003). The number of target stars per  $16.9^\circ \times 5^\circ$  DEMOS field is approximately 100. The slitlet widths were filled at  $0''.7$  to match the median seeing, and the slitlet-lengths were always larger than  $5''$ , giving access to a good estimation of the local sky.

The spectroscopic images were processed and combined using the pipeline software developed by the "DEEP" consortium. This software debiases, performs a flat-field, extracts, wavelength-calibrates and sky-subtracts the spectra. After extracting the spectra with a boxcar algorithm, the radial velocities of the stars were measured with respect to spectra of standard stars observed during the observing run. By fitting the peak of the cross-correlation function with a Gaussian, an estimate of the radial velocity accuracy was obtained for each radial velocity measurement. The accuracy of these data are astonishing for such faint stars, with typical uncertainties of  $5 \text{ km s}^{-1}$  to  $10 \text{ km s}^{-1}$ . Finally, M 31-centred radial velocities are calculated by adding  $300 \text{ km s}^{-1}$  to the Heliocentric values.

In the 4 stream fields 184 stars were measured with radial velocity uncertainties less than  $25 \text{ km s}^{-1}$ . The right-hand panel of Figure 1 shows the subset of 125 stars that

have heliocentric velocity  $v_h < 100 \text{ km s}^{-1}$ , as a function of projected distance  $d (= 780 \tan[\eta] \text{ kpc})$  along the declination direction. For clarity, stars with  $v_h > 100 \text{ km s}^{-1}$ , which are primarily Galactic, have been omitted from this diagram. These four fields correspond to CFHT Fields 1, 2, 4 and 8, and their locations on the sky are marked in the left-hand panel. The Heliocentric distances of the fields, as measured from the magnitude of the Tip of the RGB of the Stream population (McConnachie et al. 2003), are displayed in the right-hand panel of Figure 2. The outermost field lies at  $(\xi = 2.0; \eta = 4.1)$  at a Heliocentric distance of  $886 \pm 20 \text{ kpc}$ , that is, it extends out to  $125 \pm 17 \text{ kpc}$  from the centre of M 31. This is the first time that it has been possible to measure the kinematics of a stellar stream over such a huge range in galactocentric distance. An immediately striking aspect of these data is the sharp edge to the distribution at negative velocities in Figure 1, with a velocity gradient that appears to be almost a straight line. The velocity distribution near this edge is very narrow, as demonstrated by Figure 3, where we show the distribution of velocity offsets from the straight line in Figure 1. We compare the data between  $40 \text{ km s}^{-1}$  to  $40 \text{ km s}^{-1}$  in Figure 3 to a Gaussian model using the maximum likelihood technique, and find that the dispersion is  $11 \pm 3 \text{ km s}^{-1}$ . The distribution appears slightly skewed to positive velocities; defining skewness to be  $\frac{1}{N} \sum_{j=1}^N \frac{x_j - \bar{x}}{\sigma}^3$  (see e.g., Press et al. 1992), we find that the distribution of 82 stars in Figure 3 that have  $|v_j| < 100 \text{ km s}^{-1}$  have a skewness of 0.51. For comparison, the standard deviation of the skewness of samples of 82 stars drawn from a Gaussian distribution is 0.43, so the observed sample is not significantly skewed. Some of the stars in the skewed tail may be contaminants from the halo of M 31, and others may be stream stars more distant along the line of sight. The nature of these objects may become clearer when N-body simulations are fitted to the stream.

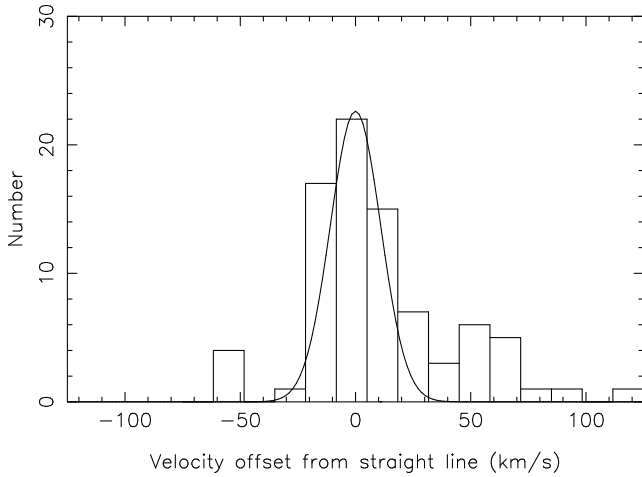


Figure 3. The distribution of velocities about the straight line displayed on the right-hand panel of Figure 1. The stream has a narrowly-peaked velocity distribution at the position of that straight line, with dispersion  $11 \pm 3 \text{ km s}^{-1}$ .

### 3 CONSTRAINTS ON THE DARK MATTER HALO

Before fitting an orbit model in a realistic galaxy potential through the position and velocity data, it is worth investigating what can be learned from a simple "back-of-the-envelope" analytic calculation. We assume that the global potential at the distance of the stream is approximated by a spherical potential, and that the stream follows the orbit of the centre of mass so all stars have the same total energy  $E = \psi(r) + \frac{1}{2}v(r)^2$ , where  $v$  is the three dimensional velocity of a star at radial position  $r$ . If we assume further that the orbit is radial, which is a reasonable approximation given the distance information in Figure 2, then  $v(r) = v(\theta) = v(\theta) \cos(\theta)$ , where  $v$  is the observed (one-dimensional) radial velocity, as a function of angular distance  $\theta = \cos^{-1}[\cos(\theta) \cos(\theta)] = \sin^{-1}[\frac{r}{780 \text{ kpc}} \sin(\theta)]$  along the stream, and  $\theta$  is the projection angle onto the line of sight. The M 31-Sun-Field 1 triangle has an angle of  $\cos^{-1}[\cos(2.0) \cos(4.1)]$ , and lengths 780 kpc (M 31-Sun), 886  $\pm$  20 kpc (Sun-Field 1), and 125  $\pm$  17 kpc (Field 1-M 31). Thus the cosine of the projection angle onto the line of sight is  $\cos(\theta) = 0.868 \pm 0.040$ . We take 2 data points ( $\theta_1 = 2.0$ ;  $v_1 = 4.1$ ) and ( $\theta_2 = 0.7$ ;  $v_2 = 1.6$ ), for which the de-projected Andromeda-centric distance and de-projected velocity are: ( $r_1 = 125 \pm 17 \text{ kpc}$ ;  $v_1 = 9 \pm 13 \text{ km s}^{-1}$ ), ( $r_2 = r_1 \sin(\theta_2) = \sin(\theta_1) = 49 \pm 18 \text{ kpc}$ ;  $v_2 = 222 \pm 13 \text{ km s}^{-1}$ ), to represent the stream. The uncertainty on  $r_1$  is calculated from the projection and distance uncertainties, while the uncertainties on  $v_1$  and  $v_2$  are estimated from the  $11 \pm 3 \text{ km s}^{-1}$  dispersion combined with the projection uncertainty. These two points correspond to the extremities of Fields 1 and 6 (we do not choose Field 8, as this region is much deeper in the potential, where the disk contribution is significant). In calculating these de-projected velocities, we have assumed that the tangential velocity of M 31 is zero. It has long been suspected that this tangential velocity is small given that there is no other large galaxy in the Local Group to provide significant torque to the Milky Way-M 31 system (Kahn & Oltjer 1959). Lynden-Bell & Lin (1977) have also pointed

out that this tangential motion must be small, as there is otherwise not enough time for M 31 and the Milky Way to have almost completed an orbit about each other in the age of the Universe, as is required by the Local Group timing argument. The result of Einasto & Lynden-Bell (1982) is consistent with this possibility; they find that the transverse motion of M 31 is  $60 \pm 30 \text{ km s}^{-1}$ , under the assumption that M 31 and the Milky Way have equal and opposite angular momenta. To provide a crude assessment of the effect of the possible transverse motion of M 31 on the parameters derived from our dataset, we also consider in the analysis below the consequence of a transverse motion of amplitude  $300 \text{ km s}^{-1}$  (i.e. equal to the radial velocity component) in the direction parallel to the Stream.

For a Kepler potential, the two chosen distance and velocity data points imply a central mass of  $4.6 \pm 0.7 \pm 0.3 \times 10^{11} M_\odot$  (the second uncertainty quantifies the effect of a  $300 \text{ km s}^{-1}$  transverse velocity). A slightly more realistic case is a logarithmic potential  $\psi = \frac{1}{2}v_c^2 \log(r_c^2 + r^2)$ , which has a circular velocity that asymptotes to  $v_c$  at large radius  $r$ . Following Dehnen & Binney (1998), we adopt a core radius of  $r_c = 3 \text{ kpc}$  for this model. In this case,

$$v_c^2 = (v_2^2 - v_1^2) \ln \frac{r_c^2 + r_1^2}{r_c^2 + r_2^2};$$

which gives a circular velocity of  $v_c = 162 \pm 15 \pm 8 \text{ km s}^{-1}$ . We also investigated a simple model in which M 31 is an NFW potential  $\psi = GM_s \log(1 + r/r_s) = r$ , where  $M_s$  is the mass within  $5.3r_s$ , and  $r_s$  is the scale radius. Assuming the characteristic relation between halo mass and concentration in a  $z = 0$  LCDM cosmology ( $c = 15 \pm 3 \pm 3 \log(M_{200} = 10^{12} M_\odot h^{-1})$  Bullock et al. (2001), we find  $M_s = 4.4 \pm 1.2 \pm 0.3 \times 10^{11} M_\odot$ , ( $M_{200} = 8.0 \pm 2.1 \pm 0.5 \times 10^{11} M_\odot$ ,  $r_{200} = 194 \pm 16 \pm 4 \text{ kpc}$ ,  $v_{200} = 136 \pm 11 \pm 3 \text{ km s}^{-1}$ ,  $r_s = 13.1 \pm 1.4 \pm 0.4 \text{ kpc}$ ). For comparison, the mass inside 125 kpc is  $7.6 \pm 1.2 \pm 0.3 \times 10^{11} M_\odot$  for the logarithmic model and  $6.4 \pm 1.3 \pm 0.3 \times 10^{11} M_\odot$  for the NFW model, respectively. The projected distance-velocity behaviour of these three toy models is compared to the velocity measurements in Figure 1. It is no surprise that the Kepler potential over-predicts the radial velocity close to M 31, but both the simple logarithmic and NFW halo models manage to approximate the stream velocity profile well.

To constrain more realistic models of the potential, we adopted a recent composite galaxy model by Klypin, Zhao & Somerville (2002), and calculate the potential due to a sum of disk, bulge and halo mass distributions. The bulge in this model has a mass of  $1.9 \times 10^{10} M_\odot$ , while the disk has a mass of  $7 \times 10^{10} M_\odot$ , and a scale length of  $5.7 \text{ kpc}$ . Fixing the disk and bulge with the Klypin, Zhao & Somerville (2002) parameters (with the further assumption that the disk scale height is  $400 \text{ pc}$ , as suggested by Gould 1994), we investigate the spherical halo models compatible with our data. Following Klypin, Zhao & Somerville (2002), we take into account the adiabatic contraction of the halo due to the settling of baryons into the disk and bulge, which alters the potential of the inner galaxy significantly.

We consider a halo of a given mass, with the appropriate concentration (Bullock et al. 2001), and compress the halo using the Klypin, Zhao & Somerville (2002) relations. We then calculate the resulting potential by multipole expansion. Using an "AMOEBA" minimization algorithm (Press

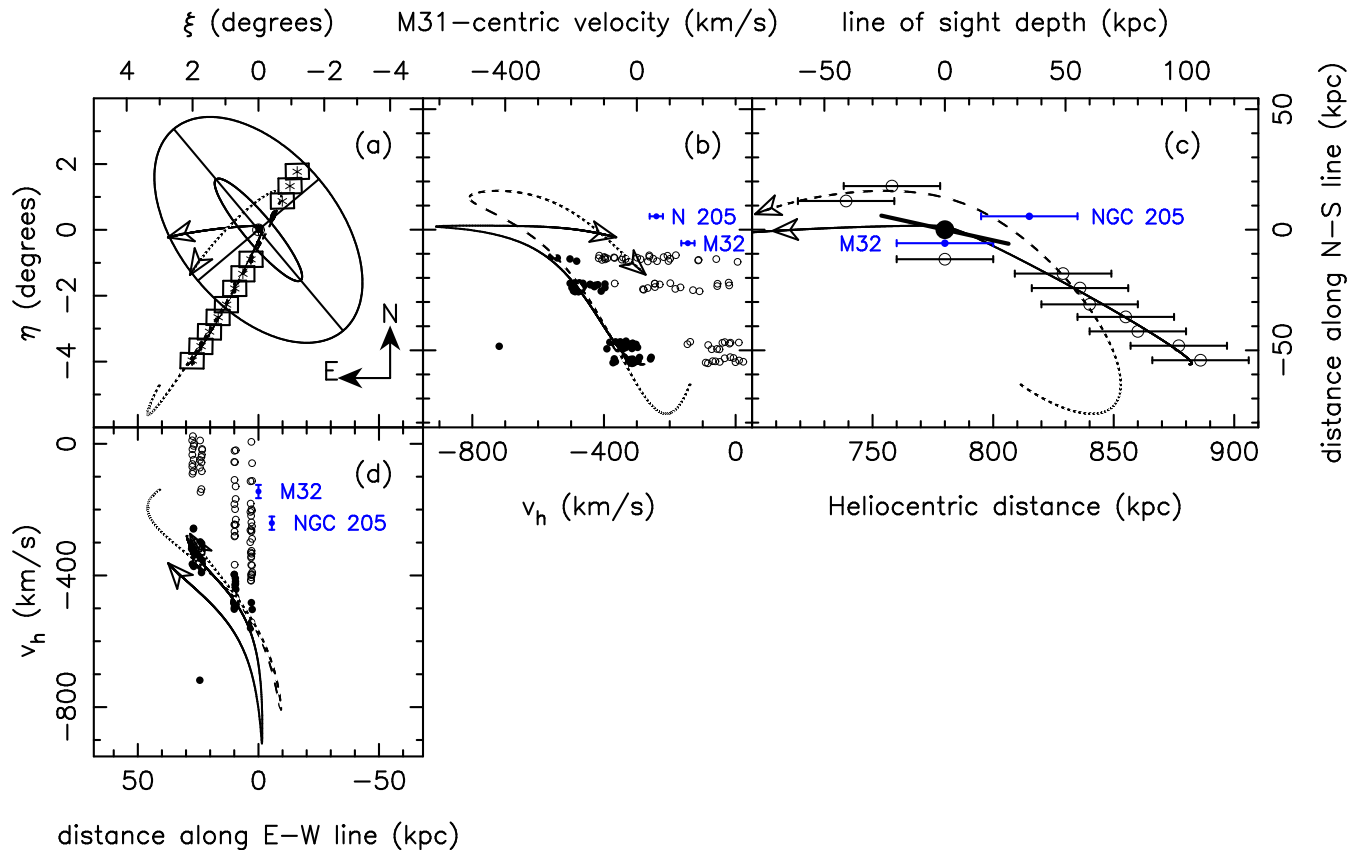


Figure 4. A multidimensional view of the two best-fitting orbits in the more realistic galaxy model of Klypin, Zhao & Somerville (2002). The kinematics in Figure 1, combined with the distance information of Figure 2, require that the stream orbit is currently moving in towards M 31, gaining velocity from Field 1 to Field 6 as the stream approaches M 31. The full line shows the orbit projection on the sky for the best-fitting orbit, in the best fitting potential, when only the data in Fields 1 (8 are taken into account; in this case the total mass of M 31 inside 125 kpc is  $M_{125} = 7.5^{+2.5}_{-1.3} \times 10^{11} M_{\odot}$ . The dashed line however, shows the best fit orbit in the best fitting potential when we also account for the distance data in Fields 12 and 13. Now the mass of the model is  $M_{125} = 1.5 \pm 0.1 \times 10^{12} M_{\odot}$  inside 125 kpc. In both cases the curves display the centre-of-mass orbits, integrated for 0.75 Gyr from the position of the centre of Field 6; the arrow heads show the direction of motion. Panel (a) shows the location on the sky of the two orbits superimposed on the chart previously shown in Figure 1; panels (b) and (d) present projections of the distance-velocity relation (symbols as in Figure 1); and finally panel (c) shows a sideways view of the orbits (as in Figure 2).

et al. 1992) we launch orbits in the potential, iteratively improving on guessed values for the initial position and velocity of a test particle on the orbit. A  $\chi^2$  goodness of fit statistic is minimized between the observed sky position, line of sight depth and radial velocity of the stars in our survey and the values predicted by the orbit model. This of course assumes that the stream follows the orbit of a test particle, an assumption that is reasonable if its progenitor was a relatively low-mass dwarf galaxy, which is consistent with the measured  $11 \pm 3 \text{ km s}^{-1}$  velocity dispersion in the stream.

We assume that the orbit must pass through the field centres on the sky to within  $0.15 \times 2 \text{ kpc}$ ; this corresponds to our estimate of the uncertainty in the measurement of the location of the central peak along the stream. To constrain the distance of the stream, we take the measurements of McConnachie et al. (2003) together with their 20 kpc distance uncertainties (these uncertainties include an estimate of the systematic error in the distance measurement). The fit is also constrained with the measured radial velocities; we take all data-points within  $100 \text{ km s}^{-1}$  of the straight-line fit in Figure 1 (those that are shown with filled circles),

and adopt the fitted velocity dispersion of  $11 \text{ km s}^{-1}$  as the expected uncertainty in the velocity.

The relative likelihood of halo mass models can be analyzed by comparing the likelihood of the orbit fit as a function of halo mass. However, we find that the result depends strongly on whether the distance data of Fields 12 and 13 are included in the fit (the stream RGB population was not detected in Field 14).

We first investigate the consequences of rejecting the distance data in Fields 12 and 13. In those fields McConnachie et al. (2003) may have detected the metal-rich thick disk, or a warp in the disk instead of the actual stream itself. Without confirmation from radial velocities, we cannot be certain that the stream continues into that area of M 31. Fitting only the data in Fields 1 to 8, we find that the most likely model has a total mass inside 125 kpc of  $M_{125} = 7.5 \times 10^{11} M_{\odot}$ ; the likelihood drops by a factor of  $e^{-1}$  (i.e. 1) for  $M_{125} = 1.0 \times 10^{12} M_{\odot}$ . We also reject at the 99% confidence level a mass lower than  $M_{125} = 5.4 \times 10^{11} M_{\odot}$ . The most likely orbit in this model galaxy potential is shown as a full line in the projections displayed in Figures 4 and

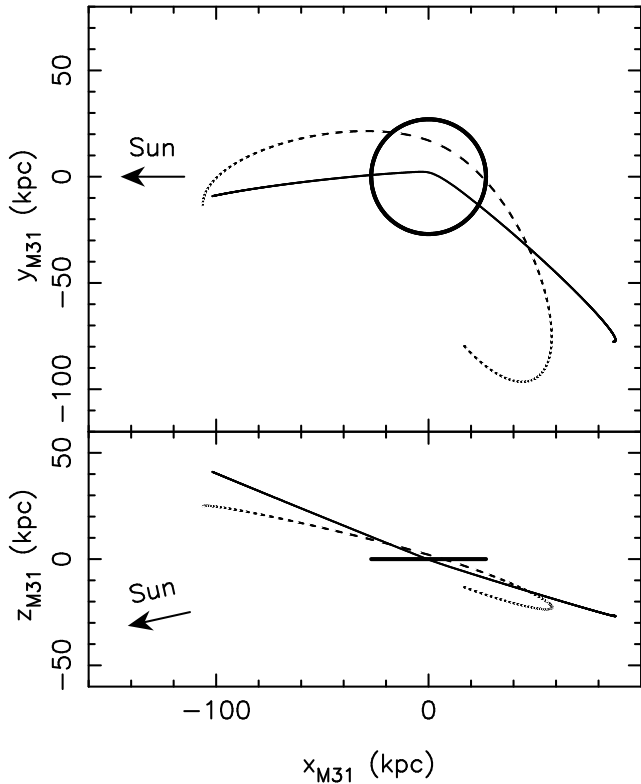


Figure 5. The paths, in M31-centric coordinates, of the two best-fitting orbits previously shown in Figure 4. In this coordinate system, the Sun is located at  $(x_{M31}; y_{M31}; z_{M31}) = (-762; 0; 169)$  kpc. The upper panel shows a face-on view of M31 (the limits of a 27 kpc radius disk is indicated with a thick circle), while the lower panel is an edge-on view of the plane of M31.

5, and its circular velocity curve is displayed in the same way in Figure 6. This orbit manages to fit the distance information in Fields 1–7 very well, but it is peculiar in being exceedingly radial (peri- to apocentre ratio of 70). Indeed, the orbit has a tangential velocity in Field 1, relative to M31, of  $5 \text{ km s}^{-1}$ , that is, the orbit has only a very small non-radial velocity component. This may be partly responsible for the good agreement of the present mass estimate with those derived above for the three toy models in which radial orbits were imposed. In the present analysis we have again assumed that the tangential motion of M31 is negligible. However, the effect of a  $300 \text{ km s}^{-1}$  tangential velocity along the direction of the Stream alters the derived mass inside 125 kpc by only  $0.5 \times 10^{11} M_{\odot}$ .

If we decide to also fit the distance data in Fields 12 and 13, the most likely model has a much higher total mass inside 125 kpc, with  $M_{125} = 1.5 \text{ }^{0.1}_{-0.25} \times 10^{12} M_{\odot}$  (again, the second uncertainty value reflects a tangential motion of M31 of  $300 \text{ km s}^{-1}$ ). The most likely orbit in this potential model is shown with a dashed line in Figures 4 and 5, and the circular velocity of the potential is shown with a dashed line in Figure 6. This orbit does not manage to fit the large line of sight distances in Fields 1 and 2 as well as the previous case (although the discrepancy is not statistically significant given the large error bars on these distance data). The main shortcoming is that the circular velocity of this model at galactocentric distances below 30 kpc is at odds with the data displayed in Figure 6. The circular velocity of the halo

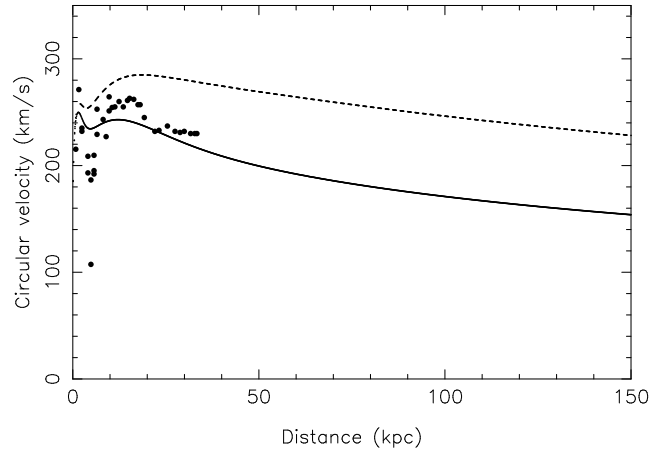


Figure 6. The circular velocity curve of the two best-fitting potentials. The high-mass model (dashed line), based on the assumption that the stream continues to Fields 12 and 13, greatly over-predicts the observed rotation curve between 20–30 kpc. The M31 rotation curve data are reproduced here with solid dots (from the compilation by Klypin, Zhao & Somerville 2002).

alone (without the bulge and disk) is higher than the data allow. This model is therefore not acceptable.

#### 4 DISCUSSION AND CONCLUSIONS

In this first kinematic study of the giant stellar stream in the Andromeda galaxy, we have been able to measure the radial velocity gradient along the stream from the outermost field currently probed, 125 kpc distant from the centre of M31, down to an inner field 20 kpc from the centre of that galaxy. Over this huge distance, the (projected) radial velocity changes by  $245 \text{ km s}^{-1}$ , implying a de-projected velocity difference of  $280 \text{ km s}^{-1}$ . This velocity gradient is used to obtain a zeroth order analytic estimate of the mass of the halo, which for simple halo-only galaxy models such as a logarithmic halo or an NFW halo, implies a mass inside 125 kpc of  $M_{125} = 7.6 \text{ }^{1.2}_{-1.3} \times 10^{11} M_{\odot}$  and  $M_{125} = 6.4 \text{ }^{1.3}_{-1.3} \times 10^{11} M_{\odot}$ , respectively. In both cases, the uncertainty associated with a possible tangential velocity of M31 of  $300 \text{ km s}^{-1}$ , is 5%.

We also investigate more realistic solutions, allowing the stream to have a non-radial orbit, and taking a galaxy model that is the sum of a disk, bulge and dark halo (Klypin, Zhao & Somerville 2002). The dark halo of this model is a perturbation on a spherical NFW model, to account for the adiabatic contraction of the dark matter as the baryonic components form. If we disregard the distance data in Fields 12 and 13, since we cannot be certain that the stream is present in those regions, the most likely mass of this galaxy model is  $M_{125} = 7.5 \text{ }^{+2.5}_{-1.3} \times 10^{11} M_{\odot}$ , with a lower limit of  $M_{125} = 5.4 \times 10^{11} M_{\odot}$  (at 99% confidence). This result is fully consistent with the zeroth order analytic estimates discussed above, and suggests that the derived mass is not very sensitive to the adopted mass model. Furthermore, there is a reasonable agreement of the resulting rotation curve with the kinematics of previously-observed disk tracers (see Figure 6), despite the fact that the model was only fit to the kinematics of the stream. This agreement is due in part to the fact that we have taken previously-fitted models for the

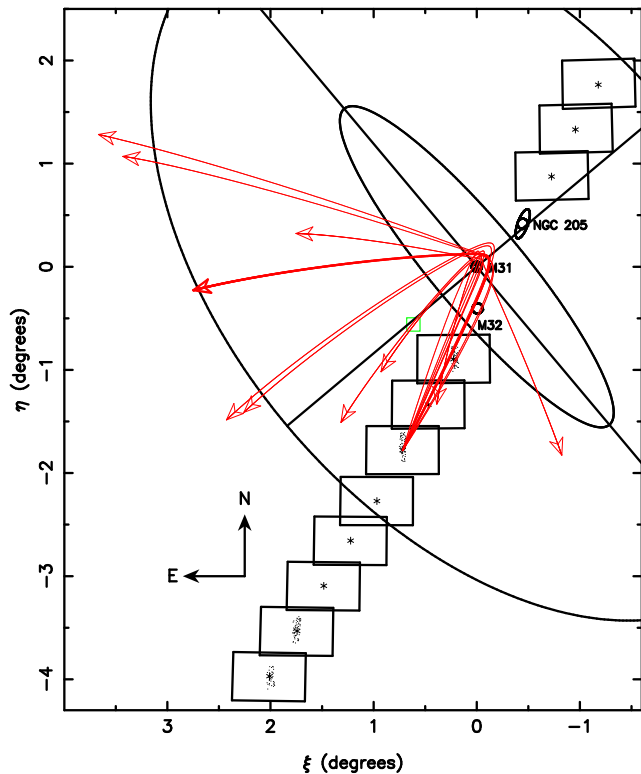


Figure 7. The spreading of orbits after a close encounter with M 31. The thick-line orbit reproduces the best-fit orbit in the realistic galaxy potential previously shown in Figure 4, integrated from the centre of Field 6. The thin-lines show similar orbits, starting from the same spatial position, but with velocities perturbed by a random offset drawn from a Gaussian distribution of dispersion  $11 \text{ km s}^{-1}$ . This fanning-out of stars on nearby orbits will lead to the disappearance of the Andromeda Stream, and implies that it is a transient phenomenon. The small squares along the minor axis show the position of the Brown et al. (2003) ACS field (not drawn to scale!). All other markings are as in Figure 1.

disk and bulge, but the halo contribution to the total rotation curve dominates beyond  $20 \text{ kpc}$ , and it is at these large distances that we have fitted the model to the stream data. This confers further confidence on the derived mass model. The uncertainty on the mass estimate due to the possible tangential velocity of M 31 is likely not very large, approximately 7% for a tangential velocity of  $300 \text{ km s}^{-1}$ . One of the main uncertainties in the present analysis is the flattening of the halo, which we have not explored, as the current data set does not provide sufficient constraints. Future studies, fitting N-body simulations to a larger kinematic sample of stream stars, can be expected to improve the mass estimate and also constrain the halo shape.

It is only recently that measurements of the mass of M 31 beyond the edge of its gaseous disk have been possible. Courteau & van den Bergh (1999) analysed the velocities of 7 Andromeda satellites, finding a total mass of  $13.3 \pm 1.8 \times 10^{11} M_{\odot}$ . In contrast, using a larger sample of 10 satellite galaxies, 17 globular clusters and 9 planetary nebulae as test particles, Evans & Wilkinson (2000) found that the most likely total mass of M 31 is  $12.3^{+1.8}_{-0.6} \times 10^{11} M_{\odot}$ , approximately half of their Milky Way estimate of  $19^{+3.6}_{-1.7} \times 10^{11} M_{\odot}$ . With improved radial velocities of the M 31 satellites they

were later able to reduce their M 31 mass uncertainties, finding a value of the total mass of  $7.0^{+10.5}_{-3.5} \times 10^{11} M_{\odot}$  (Evans et al. 2000), which is fully consistent with our result of  $M_{125} = 7.5^{+2.5}_{-1.3} \times 10^{11} M_{\odot}$  (defined within a radius of  $125 \text{ kpc}$ ). However, a definitive statement of the relative masses of M 31 and the Milky Way awaits an improved measurement for the Milky Way.

The best orbit in the best potential is prograde and in the region where it is currently observed, it lies close to the plane of M 31. Thus it appears that the orbit of the Andromeda stream is peculiar in being extremely radial, passing very close (within  $2 \text{ kpc}$ ) of the centre of M 31. This requires very special initial conditions. The stream stars, which are spatially narrowly confined in Fields 1 to 8, will diverge dramatically upon passing close to M 31 to form a low-density fan-like structure, since orbits that deviate only slightly from the orbit displayed in Figure 4 on the plunging part of their course will take very different paths after being accelerated around the centre of M 31, as demonstrated in Figure 7. The fanning-out of the stream is likely to confuse efforts to measure the metallicity and age of the M 31 halo; for instance, the recent discovery by Brown et al. (2003) of a young halo component in M 31 from main-sequence fitting of an extremely deep ACS field may be due to stream contamination (see Figure 7).

Thus the stream may be in the process of vanishing as a coherent structure, providing a supply of metal-rich stars into the halo. This also suggests that the stream was removed from its progenitor less than an orbital period ago (the pericentre to pericentre period of the continuous-line orbit in Figure 4 is  $1.8 \text{ G yr}$ ), as we would otherwise not observe the structure as a stream. The ephemeral nature of the stream implies that the progenitor must have survived until

$1.8 \text{ G yr}$  ago. As we discuss further below, the progenitor was probably of low mass, implying that the rate of decay of its orbit due to dynamical friction was slow, so it followed (or continues to follow) an orbit close to the current orbit of the stream. However, any dwarf galaxy on the derived orbit must have experienced extreme tides as it repeatedly passed close to the centre of M 31. One option is that the progenitor was a very dense dwarf galaxy that was sufficiently robust to survive the huge tides. This brings to mind M 32 as a candidate, though detailed numerical modeling is required to examine this possibility. The alternative option is that the progenitor of the stream dected off another halo object, sending it plunging into the current orbit, analogous to the suggestion by Zhao (1998) to explain the longevity of the Galactic satellite Sagittarius.

However, the connection with M 32 presents some difficulties. Although M 32 appears to reside in the stream, its velocity is markedly different. For M 32 to be associated with the stream would require it to be at a different phase in the orbit (either lagging or trailing). Furthermore, the low velocity dispersion of the stream would appear to preclude M 32 as its progenitor (which has  $v \approx 50 \text{ km s}^{-1}$  outside of the nucleus, van der Marel et al. 1994), though this cannot be confirmed without a detailed dynamical study. The case for association of NGC 205 with the stream also appears weaker given these kinematic measurements, since the best orbit does not overlap with it in phase-space. Future studies may allow us to examine this issue in more detail by following the stream beyond the region currently probed with

kinematics. The velocities of the stream stars presented here also shed light on the recent identification of a possible new companion to M 31, And V III (Morrison et al. 2003). The radial velocities of those planetary nebulae, which are located close to M 32 (see Figure 1), appear to have radial velocities consistent with an extrapolation of the Stream, as they lie close to the straight line in the right-hand panel of Figure 1. This would suggest that And V III is most likely part of the Andromeda Stream, situated in the region of highest over-density reported by Ibata et al. (2001b). However, it is interesting to note that the radial velocities of the Morrison et al. (2003) planetary nebula sample tend to increase towards the North (showing an apparent positive gradient in the right-hand panel of Figure 1), whereas the Stream stars have a negative velocity gradient. The connection between the two structures therefore merits to be examined more carefully. During the refereeing process, a study by Merritt et al. (2003) was presented which also investigates the planetary nebulae around M 31. However, though their survey has also detected PNe in a region at the base of the stream (near our Field 8), their interpretation is inconsistent with the kinematics of the stars reported here. The direction of motion of the orbit they derive is opposite to ours, and the path of their orbit, which intercepts many M 31-disk PNe is substantially different to the orbit that we have fitted. It is possible that their finding reveals the presence of another kinematic structure in Andromeda.

The majority of the stream stars that were surveyed have a narrow velocity dispersion of  $11 \pm 3 \text{ km s}^{-1}$ , though slightly skewed to positive velocities. The fact that our line of sight looks down the stream (see Figure 2), so that we probably see stars over a range of distance along the line of sight, and hence at different phases in the orbit, will tend to render the observed velocity dispersion higher than the intrinsic velocity dispersion. This indicates that the progenitor was most likely a low mass dwarf galaxy. The Milky Way satellite Sagittarius, which has a velocity dispersion of  $11 \text{ km s}^{-1}$  (Ibata et al. 1997), also has a gigantic stellar stream, but with a larger velocity dispersion of  $20 \text{ km s}^{-1}$  (Yanny et al. 2003). However, it is unclear at present whether the lower velocity dispersion measured in the Andromeda stream compared to the Sagittarius stream implies that its progenitor was of lower mass than Sagittarius, or not.

#### ACKNOWLEDGMENTS

RI would like to thank A. Klypin and H.-S. Zhao for kindly giving us their compilation of M 31 disk kinematics, and for explaining the details of their Andromeda galaxy model. The anonymous referee is thanked for comments that improved the paper. The research of AMNF has been supported by a Marie Curie Fellowship of the European Community under contract number HPMF-CT-2002-01758.

#### REFERENCES

- Brown, T., Ferguson, H., Smith, E., Kinble, R., Sweigart, A., Renzini, A., Rich, M., Vandenberg, Don A., 2003, *ApJ* 592, 17L
- Bullock, J., Kolatt, T., Sigad, Y., Somerville, R., Kravtsov, A., Klypin, A., Primack, J., Dekel, A., 2001, *MNRAS* 321, 559
- Courteau, S., van den Bergh, S., 1999, *AJ* 118, 337
- Dehnen, W. & Binney, J., 1998, *MNRAS* 294, 429
- Einasto, J., Lynden-Bell, D., 1982, *MNRAS* 199, 67
- Evans, N., Wilkinson, M., 2000, *MNRAS* 316, 929
- Evans, N., Wilkinson, M., Guhathakurta, P., Grebel, E., Vogt, S., 2000, *ApJ* 540, 9L
- Ferguson, A., Irwin, M., Ibata, R., Lewis, G., Tanvir, N., 2002, *AJ* 124, 1452
- Gould, A., 1994, *ApJ* 435, 573
- Helmi, A., White, S., 1999, *MNRAS* 307, 495
- Ibata, R., Yee, R., Gilmore, G., Irwin, M. & Suntze, N., 1997, *AJ* 113, 634
- Ibata, R., Lewis, G., Irwin, M., Totten, E. & Quinn, T., 2001, *ApJ* 551, 294
- Ibata, R., Irwin, M., Lewis, G., Ferguson, A., Tanvir, N., 2001, *Nature* 412, 49
- Ibata, R., Lewis, G., Irwin, M. & Cambray, L., 2002, *MNRAS* 332, 921
- Johnston, K., Zhao, H.-S., Spergel, D., Henquist, L., 1999, *ApJ* 512, 109L
- Johnston, K., Sackett, P., Bullock, J., 2001, *ApJ* 557, 137
- Kahn, F., Woltjer, L., 1959, *ApJ* 130, 705
- Klypin, A., Zhao, H.-S., Somerville, R., 2002, *ApJ* 573, 597
- Lynden-Bell, D., Lin, D., 1977, *MNRAS* 181, 37
- Majewski, S., Skrutskie, M., Weinberg, M. & Osthimer, J., 2003, *astro-ph/0304198*
- Malin, D., Hadley, B., 1997, *PASA* 14, 52
- van der Marel, R., Rix, H.-W., Carter, D., Franx, M., White, S., de Zeeuw, T., 1994, *MNRAS* 268, 521
- McConnachie, A., Irwin, M., Ibata, R., Ferguson, A., Lewis, G., Tanvir, N., 2003, *MNRAS* 343, 1335
- Merritt, H., Kuijken, K., Merrifield, M., Romanowsky, A., Douglas, N., Napolitano, N., Amaldi, M., Capaccioli, M., Freeman, K., Gerhard, O., Evans, N., Wilkinson, M., Halliday, C., Bridges, T., Carter, D., 2003, *astro-ph/0311090*
- Morrison, H., Harding, P., Hurley-Keller, D., Jacoby, G., 2003, *ApJ* 596, 183L
- Navarro, J., Frenk, C., White, S., 1997, *ApJ* 490, 493
- Pohlen, M., Martínez-Delgado, D., Majewski, S., Palma, C., Prida, F., Balcells, M., 2003, in "Satellites and Tidal Streams" ASP conference, La Palma, Canary Islands, 26-30 May 2003, eds, F. Prida, D. Martínez-Delgado, T. M. A. honey
- Press, W., Flannery, B., Teukolsky, S. and Vetterling, W., 1992 *Numerical Recipes* (Cambridge Univ Press, Cambridge)
- Reitzer, D., Guhathakurta, P., 2002, *AJ* 124, 234
- Stanek, K., Gammach, P., 1998, *ApJ* 503, 131L
- de Vaucouleurs, G., de Vaucouleurs, A., Corwin, H., Buta, R., Paturel, G., Fouque, P., 1991, "Third Reference Catalogue of Bright Galaxies", Springer-Verlag, Berlin Heidelberg New York
- Yanny, B., et al., 2003, *ApJ* 588, 824
- Zhao, H.-S., 1998, *AJ*, 116, 149
- Zhao, H.-S., Johnston, K., Henquist, L., Spergel, D., 1998, *A&A* 348, 49